Proposal for optical U(1) rotations of electron spin trapped in a quantum dot

Sophia E. Economou* and L. J. Sham
Department of Physics, University of California San Diego, La Jolla, California 92093-0319, USA

Yanwen Wu and D. G. Steel
The H. M. Randall Laboratory of Physics, University of Michigan, Ann Arbor, Michigan 48109, USA
(Received 6 June 2006; revised manuscript received 16 October 2006; published 14 November 2006)

We present a proposal to optically implement rotations of the electron spin in a quantum dot about the growth direction (z axis). In particular, we make use of the analytic properties of sech pulses in two-level systems to realize spin rotations about the growth direction by an arbitrary angle, for which we give an analytical expression. We propose to use this scheme to experimentally demonstrate this spin rotation. Using realistic system and pulse parameters we find the fidelity of the rotation to be more than 96% for pulses in the picosecond regime, and robust against small errors in pulse parameters. We design a feedback (adaptive) loop to correct for errors originating from unintended dynamics. The rotation is still evident—albeit with a large fidelity loss—in the ensemble case, providing the possibility of demonstration of this optical spin rotation in an ensemble of quantum dots.

DOI: 10.1103/PhysRevB.74.205415 PACS number(s): 78.67.Hc, 03.67.Lx, 42.50.Md

I. INTRODUCTION

A promising qubit candidate is the spin of an electron, trapped in a quantum dot (QD) and manipulated optically via Raman transitions involving a charged exciton (trion) state. Such a scheme combines the merits of the spin in the solid state environment (long coherence times, integrability) with advanced laser technology (speed, focusing, pulse shaping). Recently, there has been significant experimental progress towards the demonstration of the key DiVincenzo requirements for this qubit. In particular, the optical generation of spin coherence has been demonstrated[1–3] and the spin coherence time has been shown to have a lower bound of 10 ns.[1] The optically induced single-qubit rotation, however, has yet to be experimentally shown for this system. In this paper, after briefly reviewing other proposals for such a demonstration (Sec. II), we present a theoretical design of an experimental demonstration of spin rotations about the growth direction in Sec. III which lends itself more appropriately for an experimental demonstration, as it is tailored to the quantum dot Λ system. In Sec. IV we review the solution of the sech pulse in a two-level system. The spin rotation based on these pulses is presented in Sec. V. The numerical simulations are shown in Sec. VI with experimental details taken into account; fidelity loss mechanisms are discussed and quantified in Sec. VII and feedback loops are devised to correct for unintended dynamics or uncertainty in pulse parameters, in Sec. VIII. Finally, Sec. XI contains simulation of the spin rotation in an ensemble of dots.

II. REVIEW OF THE SYSTEM AND OTHER PROPOSALS

The relevant Hilbert space of the system consists of the two spin states of the trapped electron and the optically excited heavy-hole trion state. A static in-plane magnetic field splits the two spin states and defines the x direction. The growth axis of the dot is the z direction and the optical axis as well. The light used is circularly polarized along z. A peculiarity of this system is that the trion level, though spin polarized perpendicularly to the magnetic field, does not precess for fields of up to 5 T.[4] Also, the spin Zeeman splitting is typically small, on the order of tens of μeV's in GaAs (Ref. 1) and on the order of hundreds of μeV's in InAs.[5,6]

Thus we have a Λ-type system with both transitions having the same polarization and being very close in frequency, as depicted in Fig. 1. Therefore, common assumptions in Raman schemes such as polarization selectivity[7] cannot be used, whereas energy selectivity would require long pulses compared to the spin precession period. This could be an issue since the spin decoherence time should be long compared to the gate time. Moreover, when the excited state linewidth is large compared to the lower level splitting (spin Zeeman splitting)—which is the case with GaAs dots—energy selectivity is not well defined, even for long pulses.

A proposal which does not explicitly require selectivity between the two transitions is available,[8] but as will now be explained it implicitly requires long pulses when the spin Zeeman splitting is small. Specifically, in Ref. 8 two pulses with a definite phase relation are used. Both pulses act on both transitions. To remove fast oscillating terms, the condition

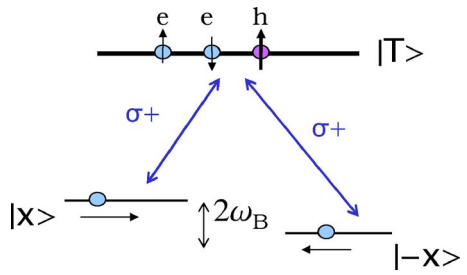

FIG. 1. (Color online) Energy levels of the three-level system, comprised by the two electron spin eigenstates of σ_x and by the trion.

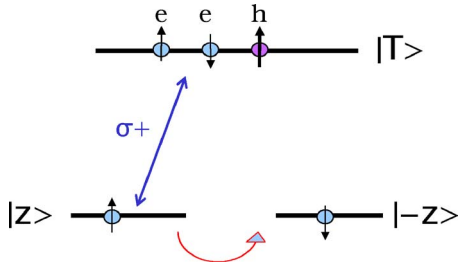

FIG. 2. (Color online) Alternative depiction of the Λ system: the two lower levels are the eigenstates of σ_z but not energy eigenstates, since they are perpendicular to the magnetic field. This basis is more suitable for imposing selection rules when circularly polarized light is used because it is just the one spin state ($|z\rangle$) that couples to the trion. The other one ($|\bar{z}\rangle$) is coupled through the magnetic field.

$$\omega_B \gg \Omega_j(t) \tag{1}$$

is imposed, where $2\omega_B$ is the spin Zeeman splitting and Ω_j is the Rabi frequency of pulse j. The axis of rotation depends on the ratio of the two Rabi frequencies and the phase between the two pulses. The angle of rotation is given by the time integral of

$$\lambda_2 = \frac{\Delta}{2} - \sqrt{\Omega_\uparrow^2 + \Omega_\downarrow^2 + \left(\frac{\Delta}{2}\right)^2}, \tag{2}$$

where Δ is the detuning. From the last relation, it is evident that in order to achieve large rotation angles, long pulses are needed, since the Rabi frequency is bounded from Eq. (1).

Another proposal[9] suggested to use a π pulse to populate the trion state for some time, during which the precession of the spin is used so that the $|\bar{z}\rangle$ state acquires a phase and subsequently a second π pulse recovers the $|z\rangle$ state population by stimulated emission. This method of rotating requires populating the trion state for a significant amount of time, so that trion decay will significantly deteriorate the fidelity. The operation will moreover be slowed down when the spin Zeeman splitting is small. It also provides a scheme for rotations only about the growth axis.

III. PROPOSAL OF ROTATIONS ABOUT Z

In the current proposal, contrary to the use of any kind of selectivity between the two transitions, we choose a pulse with sufficient bandwidth to act on both transitions. The Hamiltonian in the $\{|\bar{z}\rangle, |z\rangle, |\mathcal{T}\rangle\}$ basis has the form

$$H = \begin{bmatrix} 0 & \omega_B & 0 \\ \omega_B & 0 & \Omega(t)e^{i\omega_0 t} \\ 0 & \Omega(t)e^{-i\omega_0 t} & \epsilon_T \end{bmatrix}. \tag{3}$$

It is evident from the above form of the Hamiltonian, that the pulse only couples the $|z\rangle$ state to the excited trion state. The $|\bar{z}\rangle$ state is indirectly coupled through the B field, as shown schematically in Fig. 2. Therefore, for small spin Zeeman splitting compared to the pulse bandwidth we can view in our qualitative discussion the three-level system as two systems of dimensions 2 and 1, consisting of $\{|z\rangle, |\mathcal{T}\rangle\}$ and $\{|\bar{z}\rangle\}$,

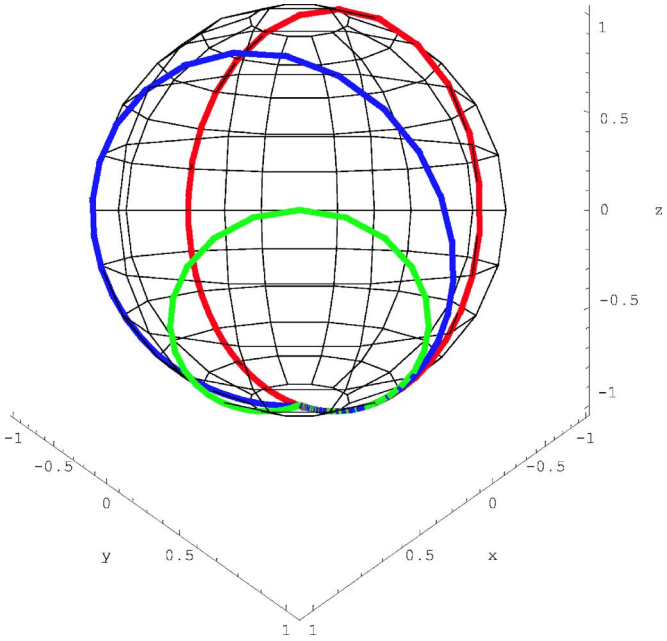

FIG. 3. (Color online) Bloch vector representation of the pseudospin; The pulse bandwidth is fixed (σ=1) and the detuning varies: Δ=0 [red (dark grey) curve], Δ=1 [blue (black) curve] and Δ=0.5 [green (light grey) curve]. The plot is in the rotating frame of the laser, not that of the unperturbed system.

respectively. This of course is an approximation, strictly valid only in the $B \to 0$ limit. For finite B we really have two two-level systems sharing a common state. Clearly, fast resonant pulses of area 2π and arbitrary pulse shape will induce a minus sign to the $|z\rangle$ relative to the $|\bar{z}\rangle$ state, due to the SU(2) character of the pseudospin. This amounts to a π rotation of the spin about z.[3,10] We propose the use of analytically solvable off-resonant 2π pulses to design rotations about z by an *arbitrary* angle, for which we provide an analytical expression.

It is well known that for a two-level system the sech pulse shape of Rosen and Zener[11] (RZ) yields an exactly solvable evolution, for arbitrary detuning. As was more recently shown, the RZ pulse belongs to a class of exactly solvable pulse shapes.[12] In what follows, we will make use of the properties of the RZ pulses in the context of the three-level system to design z rotations.

IV. REVIEW OF THE ROSEN-ZENER SOLUTION

Consider a two-state system, initially in the ground state, $|g\rangle$, with the two levels coupled by a time dependent Hamiltonian with a sech envelope and central frequency ω_o:

$$\Omega \,\mathrm{sech}(\sigma t) e^{i\omega_0 t} \equiv f(t) e^{i\omega_0 t}, \tag{4}$$

where Ω is the Rabi frequency, σ is the bandwidth of the pulse. Moving to the interaction picture, the problem reduces to solving two coupled first order equations or, equivalently, one second order equation of the form

$$\ddot{c}_e + (i\Delta - \dot{f}/f)\dot{c}_e + f^2 c_e = 0, \tag{5}$$

where c_g (c_e) is the coefficient of the ground (excited) state, Δ is the detuning, and with the initial condition $c_e(-\infty)=0$. By the change of variable

$$\zeta = \frac{1}{2}[\tanh(\sigma t) + 1], \tag{6}$$

RZ bring the equation into the form of the hypergeometric equation, where

$$a = \frac{\Omega}{\sigma}, \tag{7}$$

$$c = \frac{1}{2}\left(1 + i\frac{\Delta}{\sigma}\right). \tag{8}$$

After imposing the initial conditions, the coefficients of the ground ($|g\rangle$) and excited ($|e\rangle$) states are

$$c_g = F(a, -a, c^*, \zeta), \tag{9}$$

$$c_e = -i\frac{a}{c^*}\zeta^{1-c}F(a+1-c, 1-a-c, 2-c, \zeta). \tag{10}$$

We see from Eq. (10) and by use of the properties of the hypergeometric function that when

$$\sigma = \Omega \tag{11}$$

there is no population transfer to the excited state for $t \to \infty$, i.e., $c_e(\infty)=0$, and instead the pseudospin vector undergoes a full cycle from $|g\rangle$ to $|e\rangle$ and back to $|g\rangle$ with the ground state having acquired a phase factor

$$c_g(\infty) = -\frac{\sigma + i\Delta}{\sigma - i\Delta} \equiv e^{-i\phi}, \tag{12}$$

$$\tan\phi = \frac{2\sigma\Delta}{\Delta^2 - \sigma^2}. \tag{13}$$

For σ fixed, the path will be determined by the detuning, as shown in Fig. 3.

V. USE OF RZ PULSES FOR RAMAN QUBIT ROTATION

For an arbitrary sech pulse, the evolution operator of the whole three-level system, under the approximation of slow precession $\omega_B \ll \sigma$ is given by

$$U \simeq \begin{bmatrix} 1 & 0 & 0 \\ 0 & F(a,-a,c^*,\zeta) & -\frac{ia}{c}\zeta^c F(a+c,-a+c,1+c,\zeta) \\ 0 & -\frac{ia}{c^*}\zeta^{c^*}F(a+c^*,-a+c^*,1+c^*,\zeta) & F(a,-a,c,\zeta) \end{bmatrix}. \tag{14}$$

To have a unitary operation, it is necessary that Eq. (11) is satisfied, i.e., the trion state gets only virtually excited. We will refer to such pulses as "transitionless." Mathematically, this translates to $a=1$. We are also only interested in the form of U after the passage of the pulse, when $z=1$. Then U becomes

$$U \simeq \begin{bmatrix} 1 & 0 & 0 \\ 0 & 1-1/c^* & 0 \\ 0 & 0 & 1-1/c \end{bmatrix} \equiv \begin{bmatrix} 1 & 0 & 0 \\ 0 & e^{-i\phi} & 0 \\ 0 & 0 & e^{i\phi} \end{bmatrix}. \tag{15}$$

The truncated evolution operator, in the 2×2 spin space is described by the unitary matrix

$$U_{\text{spin}} \simeq \begin{bmatrix} 1 & 0 \\ 0 & e^{-i\phi} \end{bmatrix} = e^{-i\phi/2}\begin{bmatrix} e^{i\phi/2} & 0 \\ 0 & e^{-i\phi/2} \end{bmatrix}. \tag{16}$$

A phase between the $|z\rangle$ and $|\bar{z}\rangle$ states translates to a rotation about the z axis by an angle ϕ. So, while for a true two-level system the induced phase of a transitionless pulse is trivial when all the population is initially in the $|z\rangle$ state, for the three-level system it yields a nontrivial rotation about the z axis. The expression for the angle of rotation may be simplified:

$$\tan\frac{\phi}{2} = \frac{\sin\phi}{1+\cos\phi} = \frac{\sigma}{\Delta} \Rightarrow \phi = 2\arctan\frac{\sigma}{\Delta}. \tag{17}$$

VI. NUMERICAL SIMULATION AND EXPERIMENTAL PROPOSAL

Equations (16) and (17) are our main theoretical results. To check how well this theory works for actual three level systems and with decoherence and unintended dynamics included, we simulate the spin beats of an optical experiment in the dots.

The optical experiments on quantum dots are usually performed at 4 K, which is well above the spin Zeeman splitting for GaAs.[1,13] We are thus starting with a completely mixed state of the qubit and initializing it with optical pumping.[1] We propose to use an RZ pulse which will probabilistically initialize the spin to −0.5 polarization, as in Ref. 3. A σ+ polarized pulse creates a spin vector (SV) initially pointing

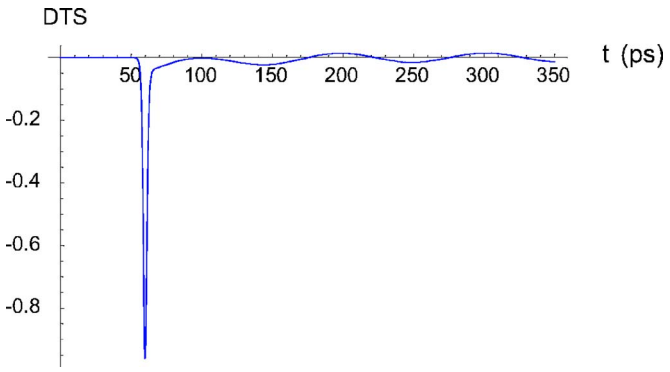

FIG. 4. (Color online) Differential transmission signal (DTS) of transitionless pulse on mixed state. Virtually no beats are generated when $\Omega=\sigma$. Here, $\sigma=0.4$ meV and $\Delta=0$.

along $-z$ and precessing about the static B field. We see that by setting $\Omega=\sigma/2$ and $\Delta=0$ all the population of the $|z\rangle$ state is transferred to the trion, which subsequently decays incoherently to the two lower states provided that the trion state linewidth is small compared to the spin Zeeman splitting so that spontaneously generated coherence (SGC)[1,14] may be ignored. In Sec. VII we will investigate the effect of SGC along with the other deteriorating mechanisms. We also stress that SGC has been taken into account in all our numerical simulations.

Since the designed operation is a rotation about the z axis, the SV should not be affected when the incident control pulse finds it at a dip or peak, i.e., at $|\bar{z}\rangle$ or $|z\rangle$, respectively. On the other hand, the most prominent effect should be when the SV is pointing along the y direction, which is the case in our simulations.

To experimentally achieve a transitionless pulse, the Rabi frequency of the initializing pulse could be doubled or preferably a separate pump-probe experiment with the control pulse in place of the pump may be performed. The transitionless pulse induces a large initial spike and then the spin beats essentially vanish, as shown in Fig. 4. The physics is simple: the transitionless pulse only virtually excites the trion, ideally transferring no population, so that it may not be used for initialization via optical pumping. Once the pulse duration and Rabi frequency of the control pulse are fixed, the detuning will be varied from $\Delta=0$, which renders a π rotation, to $\Delta=\sigma/\tan(\pi/8)$, which yields a $\pi/4$ rotation.

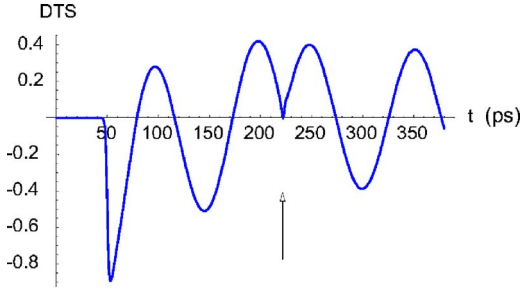

FIG. 5. (Color online) Differential transmission signal (DTS) representing rotation of the spin in a GaAs dot by π with a resonant pulse of $\sigma=0.4$ meV. The time where the control pulse is centered is indicated by the arrow.

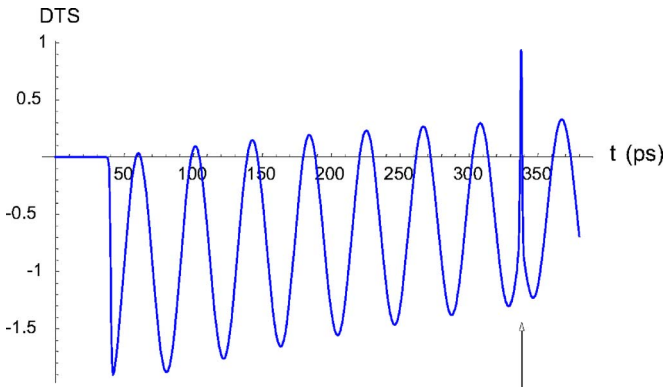

FIG. 6. (Color online) DTS representing rotation of the spin in a InAs dot by π. The pulse is resonant with $\sigma=0.8$ meV. The arrow indicates the incidence time of the control pulse.

In our simulations we have used two or three pulses: an initializing pulse, a control pulse, and in the case of $\phi\neq\pi$ a second control pulse to recover the beats and prove unitarity. Experimentally, a third (or fourth) pulse, the probe, will be used to perform the measurement of the spin. The time re-

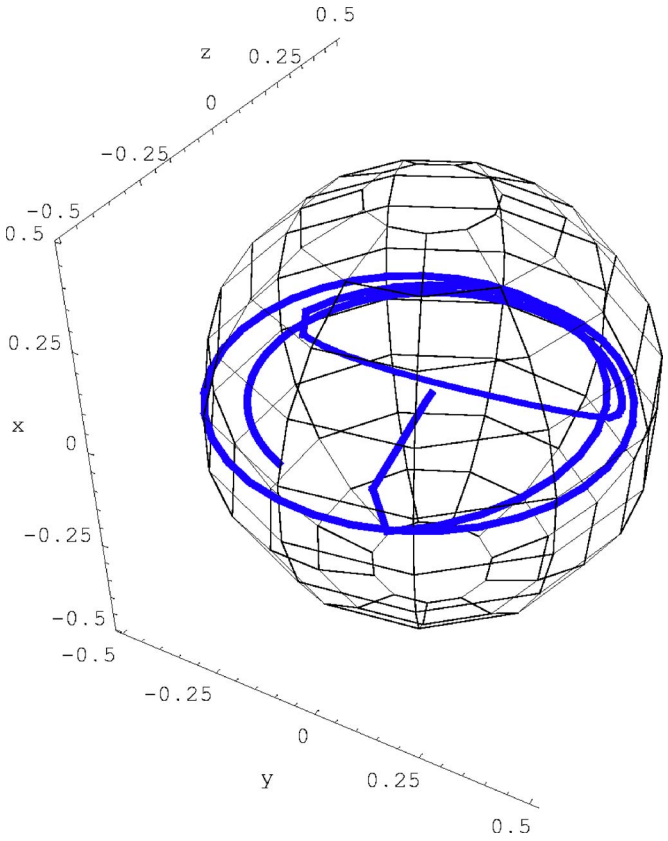

FIG. 7. (Color online) Bloch sphere depiction of the spin generation and rotation of Fig. 5. Initially there is no SV, and its generation along the $-z$ direction is shown. During the rotation the population is moved outside the 2×2 spin subspace and the SV shrinks (line inside the sphere, corresponding to the arrow of Fig. 5). The π rotation about the z axis is implemented when the SV is pointing along $-y$. Note that the Bloch sphere itself has been shrunk to a radius of 0.5 for clearer depiction.

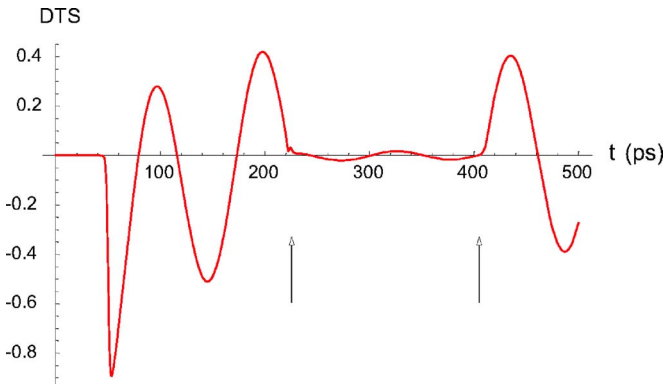

FIG. 8. (Color online) Differential transmission signal (DTS) representing spin rotation in a GaAs dot by $\pi/2$ with pulse of $\sigma=0.4$ meV and $\Delta=\sigma$. The pump is centered at 50 ps, when the beats start and the central times of the control pulses are indicated by the arrows.

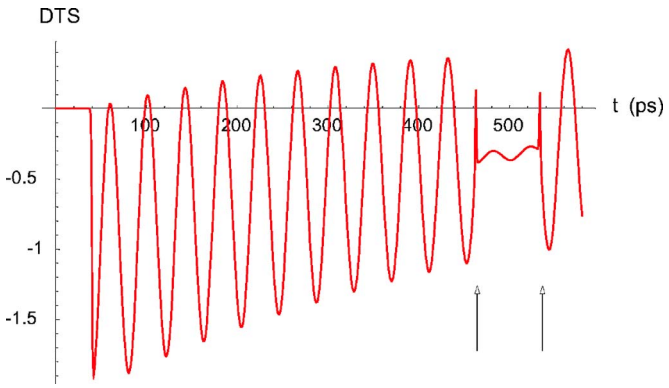

FIG. 9. (Color online) DTS showing the rotation of the spin in a InAs dot by $\pi/2$. The pulse parameters are $\sigma=\Delta=0.8$ meV. The arrows indicate the incidence time of the two control pulses.

solved probe signal is called the differential transmission signal (DTS) as it measures the difference between the probe signal with the pump on and that with the pump off. When both a co-circularly and cross-circularly polarized probe is used and the difference is taken[1] the quantity measured is $\rho_{zz}-\rho_{\mathcal{T}\mathcal{T}}-\rho_{\bar{z}\bar{z}}+\rho_{\bar{\mathcal{T}}\bar{\mathcal{T}}}$. For a $\sigma+$ polarized pump, as in our case, and after the decay of the trion level ($\rho_{\mathcal{T}\mathcal{T}}=0$) the quantity measured is $\rho_{zz}-\rho_{\bar{z}\bar{z}}$, i.e., the z component of the SV. The duration of the pulses is taken to be about 6 ps for GaAs, close to those used in Ref. 1, which translates to about $\sigma=0.4$ meV. We take the spin Zeeman splitting to be 40 μeV, which corresponds to a B field of about 6.5 T.[1] For InAs dots, we take $\sigma=0.8$ meV and the spin Zeeman splitting to be 0.1 meV, which corresponds to $B\sim 2.3$ T.[6] The trion decay rate for GaAs is also taken from Ref. 1, equal to 0.01 meV. For InAs dots it is about 0.6 μeV.[15] The spin dephasing has been chosen conservatively equal to 0.5 μeV for both kinds of dots.

For a π rotation of the spin, the degree of unitarity of the operation is evident in the beat amplitude after the control pulse, Figs. 5 and 6 for GaAs and InAs dots, respectively. In Fig. 7 a Bloch vector illustration of the spin generation and π rotation (corresponding to Fig. 5) is shown. To demonstrate the unitarity of the control pulse for a rotation angle other than π, a second control pulse is used to rotate the SV back to the yz plane and thus recover the initial beat amplitude, as shown in Fig. 8 for GaAs and in Fig. 9 for InAs. We note that the beats are not recovered completely due to errors originating from the trion decay and the (small but finite) precession of the spin during the operation. We will ignore spin dephasing in the following discussion on fidelity.

The spin will be measured via a weak probe. Given that a $\sigma+$ polarized probe measures the z component of the SV, the actual angle of rotation in the experiment will be given by

$$\phi_{\text{exp}} = \arccos \frac{A_1}{A_0}, \tag{18}$$

where A_0 and A_1 are the beat amplitudes before and after the control pulse respectively, as in Ref. 16.

VII. FIDELITY

A. Initialization

The initialization process described above ideally yields a 50% fidelity. However, the mechanism that undermines the fidelity of the initialization is SGC, as mentioned above.[14] SGC is suppressed by making the spin Zeeman splitting larger.[1,14] Our numerical simulations show that the fidelity of initialization is about 40% for GaAs, even for relatively large Zeeman splittings. Since the initialization is far from perfect anyway, we will not worry about SGC effects.

A more important issue is a possible uncertainty in the Rabi frequency, stemming from limited knowledge of the dipole matrix element between $|z\rangle$ and $|t\rangle$. Deviation of the Rabi frequency from $\sigma/2$ will limit the generated polarization. In Sec. VIII we discuss how to maximize the polarization by use of adaptive feedback loops.

Finally, valence band mixing will affect the spin polarization by altering the selection rules. Again, by use of a feedback loop that scans through the polarization of the laser, a true Λ configuration is reached. This, also discussed in Sec. VIII, will also allow for correction due to valence band mixing in the subsequent control of the spin.

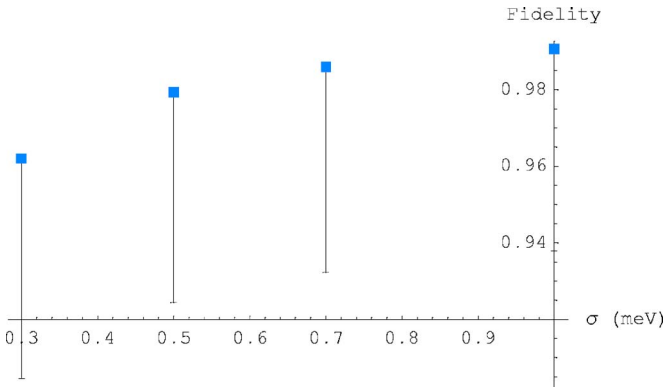

FIG. 10. (Color online) Fidelity of the operation as a function of the pulse bandwidth for GaAs dots. Large bandwidth corresponds to fast pulses, and therefore smaller time intervals of trion excitation. Here the angle of rotation equals π. The uncertainty in the laser electric field is 15%.

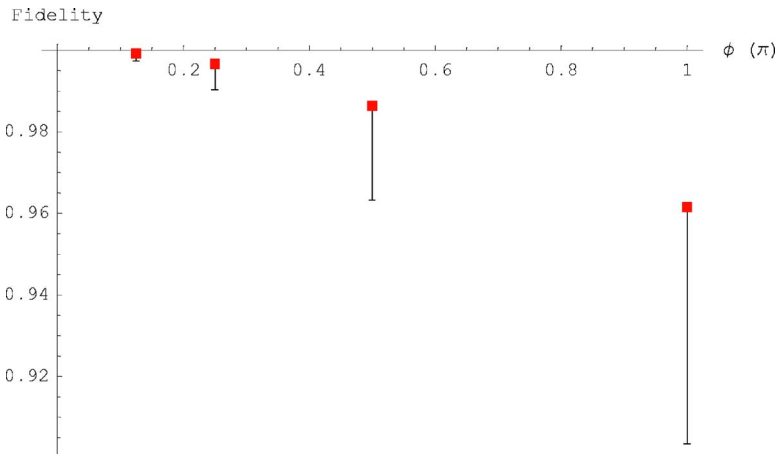

FIG. 11. (Color online) Fidelity of the operation as a function of the angle of rotation for GaAs dots. Large angles correspond to pulses closer to resonance, yielding loss of fidelity due to (real) trion excitation. Here the bandwidth has been taken equal to 0.3 meV and the uncertainty in the laser electric field is 15%.

B. Rotation

The fidelity is given by[16,17]

$$\mathcal{F} = \overline{|\langle \Psi | \tilde{U}^{\dagger} U_{id} | \Psi \rangle|^2}, \tag{19}$$

where Ψ is the initial state, $\tilde{U}$ and U_{id} are the actual and ideal operations, respectively, and the average is to be taken over the relevant (in our case 2×2) Hilbert space. If we define

$$I = \tilde{U}^{\dagger} U_{id}, \tag{20}$$

then the fidelity becomes

$$\mathcal{F} = \frac{1}{3} \sum_i |I_{ii}|^2 + \frac{1}{6} \sum_{i \neq j} |I_{ij}|^2. \tag{21}$$

The purity of the operation is given by[17]

$$\mathcal{P} = \overline{\mathrm{Tr}(\rho_{\mathrm{out}}^2)} = \frac{1}{3} \sum_i \mathrm{Tr} R_{ii}^2 + \frac{1}{6} \sum_{i \neq j} \mathrm{Tr}(R_{ii} R_{jj} + R_{ij} R_{ji}), \tag{22}$$

where $R_{ij} = \tilde{U} \rho_{ij} \tilde{U}^{\dagger}$.

The fidelity of the operation deteriorates due to the following mechanisms: the decay of the trion state during the optical pulse, the spin precession during the pulse action, and the spin dephasing. The dominant mechanism is the former; it is irreversible and will degrade the unitarity of the operation, with the effect being stronger for longer pulses and for pulses closer to resonance. Obviously, the shorter the pulse the higher the fidelity; however, there may be a lower bound to how short a pulse can be, as there seems to be an upper bound on pulse strength the system can accommodate. Figure 10 shows the fidelity as a function of the pulse bandwidth. Smaller detunings correspond to larger rotation angles, Eq. (17), so that the fidelity is lower for large rotation angles, and is close to perfect for small angles, as shown in Figs. 11 and 12 for GaAs and InAs dots, respectively.

On the other hand, the precession of the spin vector during the action of the control pulse is a reversible evolution, and will not affect the purity of the operation. It will, however, cause a tilt to the axis of rotation, affecting the fidelity. In principle, this can be taken into account by choosing this alternate axis of rotation instead of insisting on rotations about z. In our case, however, it does play a small role in the loss of fidelity, more so for longer pulses.

As in the initialization case, uncertainty in the Rabi frequency and valence band mixing will affect the fidelity of the rotation. In the next section we discuss how to overcome these effects by use of feedback loops. Once this process is carried out for initialization, the appropriate pulses will automatically be known for the rotation.

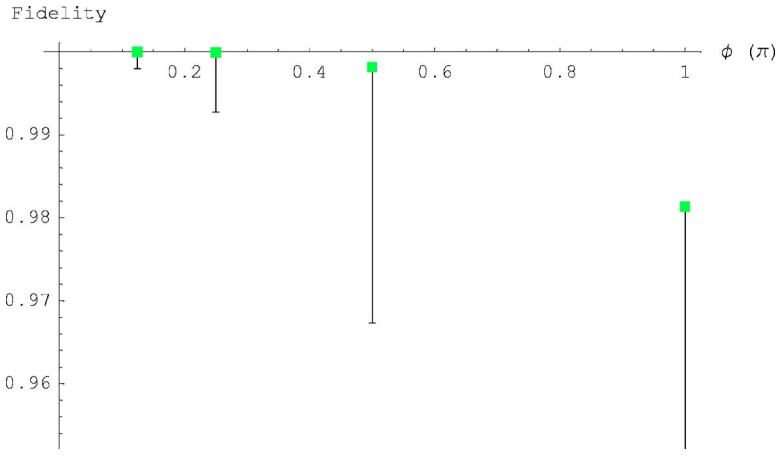

FIG. 12. (Color online) Fidelity of the operation as a function of the angle of rotation for InAs dots. Large angles correspond to pulses closer to resonance, yielding loss of fidelity due to (real) trion excitation. Here the bandwidth has been taken equal to 0.8 meV. The uncertainty in the laser electric field is 15%.

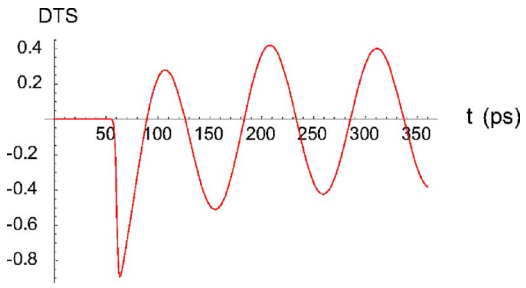

FIG. 13. (Color online) Initialization using a sech pulse with σ=0.4 meV and $\Omega=\sigma/2$.

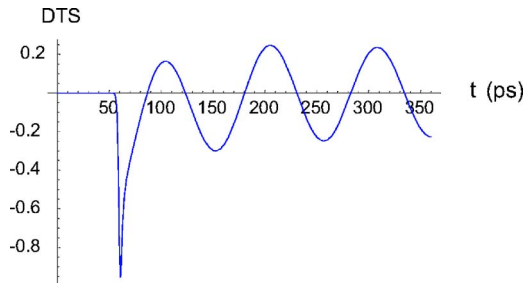

FIG. 14. (Color online) Initialization with a pulse with σ =0.4 meV and $\Omega=1.5\ \sigma/2$.

VIII. OVERCOMING ERRORS WITH FEEDBACK LOOPS

A. Uncertainty in laser parameters

Experimentally, the Rabi frequency may not be exactly known if the polarization matrix element between $|z\rangle$ and $|\mathcal{T}\rangle$ has not been measured; one way to find the optimal value of the Rabi frequency is fixing the pulse duration and scanning the intensity until the response (spin polarization) is maximized. Actually, even if the pulse duration is not precisely known, we can devise a feedback loop which combined with the analyticity of our solution will yield the maximum polarization, i.e., will pick the pulse with $\Omega=\sigma/2$. By use of the evolution operator of Eq. (14), we can find the trion population after the passage of the pulse. The truncated evolution operator for time $t\to\infty$ and for resonant pulses takes the form

$$\Lambda(\Delta=0)\simeq\begin{bmatrix}1 & 0\\ 0 & \cos\left(\frac{\Delta\theta}{2}\right)\end{bmatrix}, \tag{23}$$

where $\Delta\theta=2\pi\frac{\Omega}{\sigma}$ is the pulse area. Action of Λ on a mixed density matrix yields

$$\rho=\begin{bmatrix}1/2 & 0\\ 0 & 1/2\cos^2\left(\frac{\Delta\theta}{2}\right)\end{bmatrix}. \tag{24}$$

The feedback loop we propose consists of the laser, which is connected to a computer which also records the measurements from each run, and a pulse shaper. The pulse bandwidth is fixed but not precisely known. The initial value of the Rabi frequency (laser power) is also unknown, call it Ω_1. After the trion decays, the signal is proportional to the spin polarization. The maximum of the beats then is given by

$$P_1=\frac{A}{2}\sin^2\left(\frac{\Omega_1}{\sigma}\pi\right), \tag{25}$$

where A is some unknown constant related to the measurement process. The value P_1 is recorded and in the next run the Rabi frequency is doubled, $\Omega_2=2\Omega_1$. The next run will thus yield

$$P_2=\frac{A}{2}\sin^2\left(\frac{2\Omega_1}{\sigma}\pi\right). \tag{26}$$

The ratio is

$$P_1/P_2=\frac{\sin^2\left(\frac{\Omega_1}{\sigma}\pi\right)}{\sin^2\left(\frac{2\Omega_1}{\sigma}\pi\right)}\Rightarrow\sqrt{\frac{P_2}{P_1}}=\cos\left(\frac{\Omega_2\pi}{2\sigma}\right)\Rightarrow\Omega_2$$
$$=\frac{\sigma}{2\pi}\arccos\left(\frac{1}{2}\sqrt{\frac{P_2}{P_1}}\right). \tag{27}$$

Therefore, in the third run the Rabi frequency should be chosen to be

$$\Omega_3=\frac{\pi\Omega_2}{\arccos\left(\frac{1}{2}\sqrt{\frac{P_2}{P_1}}\right)}, \tag{28}$$

which is the target value, $\sigma/2$. This is the maximum SV that can be generated at a single shot, shown in Fig. 13 (compare to Figs. 14 and 15 for a stronger and weaker pulse, respectively). An advantage of this scheme is that knowledge of neither the pulse duration nor the Rabi frequency are required. It is also an indirect way of determining the dipole matrix element between $|z\rangle$ and $|\mathcal{T}\rangle$.

B. Finite valence band mixing

In the presence of valence band mixing, the Hilbert space is no longer 3×3. We account here for mixing between the $|\frac{3}{2}\rangle$ ($|\overline{\frac{3}{2}}\rangle$) and the $|\frac{1}{2}\rangle$ ($|\overline{\frac{1}{2}}\rangle$) trions. Since in all cases the electrons are in the same orbital and in a spin singlet state, we list only the hole states

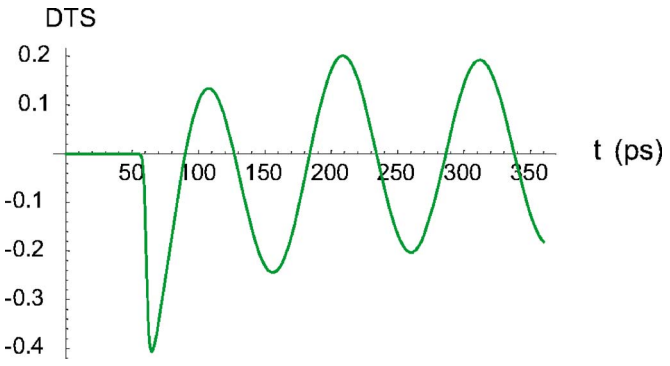

FIG. 15. (Color online) Initialization with a pulse with σ =0.4 meV and $\Omega=0.5\ \sigma/2$.

$$|HH+\rangle = -\frac{1}{\sqrt{2}}|(X+iY)\uparrow\rangle, \tag{29}$$

$$|LH-\rangle = \frac{1}{\sqrt{6}}|(X-iY)\uparrow\rangle + \sqrt{\frac{2}{3}}|Z\downarrow\rangle, \tag{30}$$

$$|LH+\rangle = -\frac{1}{\sqrt{6}}|(X+iY)\downarrow\rangle + \sqrt{\frac{2}{3}}|Z\uparrow\rangle, \tag{31}$$

$$|HH-\rangle = \frac{1}{\sqrt{2}}|(X-iY)\downarrow\rangle, \tag{32}$$

where $|X\pm iY\rangle$ and $|Z\rangle$ are the $l=1$ spherical harmonics with $m=\pm 1$ and $m=0$, respectively. The corresponding trion states will be denoted by $|H\rangle$ $(=|\mathcal{T}\rangle)$, $|\bar{L}\rangle$, $|L\rangle$, $|\bar{H}\rangle$.

When valence band mixing is included, the valence Hamiltonian in the $\{|H\rangle, |\bar{L}\rangle, |H\rangle, |L\rangle\}$ basis is

$$H = \begin{bmatrix} \epsilon_H & v & 0 & 0 \\ v^* & \epsilon_L & 0 & 0 \\ 0 & 0 & \epsilon_H & v \\ 0 & 0 & v^* & \epsilon_L \end{bmatrix}, \tag{33}$$

where v is the coupling between heavy and light hole. The dot potential has been assumed such that the mixing between $|H\rangle$ $(|\bar{H}\rangle)$ and $|L\rangle$ $(|\bar{L}\rangle)$ is zero. To solve the eigenvalue equation, it helps to redefine the zero of energy by subtracting $\bar{\epsilon}/2 \equiv \frac{\epsilon_L+\epsilon_H}{2}$; then we get

$$H = \begin{bmatrix} -a & v & 0 & 0 \\ v^* & a & 0 & 0 \\ 0 & 0 & -a & v \\ 0 & 0 & v^* & a \end{bmatrix}, \tag{34}$$

where $a=\frac{\epsilon_L-\epsilon_H}{2}$.

By diagonalizing within the blocks, the solution is given by the following eigenvalues and eigenstates:

$$\lambda_\pm = \pm\sqrt{a^2+v^2}, \tag{35}$$

$$C_{1,-} = \begin{bmatrix} \cos\frac{\psi}{2} \\ -\sin\frac{\psi}{2} \\ 0 \\ 0 \end{bmatrix} \equiv |H\bar{l}\rangle, \tag{36}$$

$$C_{1,+} = \begin{bmatrix} \sin\frac{\psi}{2} \\ \cos\frac{\psi}{2} \\ 0 \\ 0 \end{bmatrix} \equiv |\bar{L}h\rangle, \tag{37}$$

$$C_{2,-} = \begin{bmatrix} 0 \\ 0 \\ \cos\frac{\psi}{2} \\ -\sin\frac{\psi}{2} \end{bmatrix} \equiv |H\bar{l}\rangle, \tag{38}$$

$$C_{2,+} = \begin{bmatrix} 0 \\ 0 \\ \sin\frac{\psi}{2} \\ \cos\frac{\psi}{2} \end{bmatrix} \equiv |\bar{L}h\rangle. \tag{39}$$

The angle ψ is defined through

$$\cos\psi = \frac{a}{\sqrt{a^2+v^2}}, \tag{40}$$

and v is taken to be real.

Restoring the zero of energy, we can write the Hamiltonian in the new basis $\{|H\bar{l}\rangle, |\bar{L}h\rangle, |\bar{H}l\rangle, |L\bar{h}\rangle\}$ as

$$H = \begin{bmatrix} \frac{\bar{\epsilon}}{2}-\lambda & 0 & 0 & 0 \\ 0 & \frac{\bar{\epsilon}}{2}+\lambda & 0 & 0 \\ 0 & 0 & \frac{\bar{\epsilon}}{2}-\lambda & 0 \\ 0 & 0 & 0 & \frac{\bar{\epsilon}}{2}+\lambda \end{bmatrix}. \tag{41}$$

If $\sigma+$ light is used, propagating along z and centered at the HH trions (with energy $\frac{\bar{\epsilon}}{2}-\lambda$) the trion states of higher energy can be ignored by frequency selectivity. In the presence of the mixing we will have a 4×4 Hamiltonian instead of the 3×3 from the previous sections, where mixing was ignored. In the $\{|z\rangle, |\bar{z}\rangle, |H\bar{l}\rangle, |\bar{H}l\rangle\}$ basis, where state $|H\bar{l}\rangle$ $(|\bar{H}l\rangle)$ represents a state with largest contribution from the $|H\rangle$ $(|\bar{H}\rangle)$ the total Hamiltonian, including the dipole interaction, is

$$H_4 = \begin{bmatrix} 0 & \omega_B & \Omega\cos\frac{\psi}{2} & 0 \\ \omega_B & 0 & 0 & \frac{1}{\sqrt{3}}\Omega\sin\frac{\psi}{2} \\ \Omega^*\cos\frac{\psi}{2} & 0 & \frac{\bar{\epsilon}}{2}-\lambda & 0 \\ 0 & \frac{1}{\sqrt{3}}\Omega^*\sin\frac{\psi}{2} & 0 & \frac{\bar{\epsilon}}{2}-\lambda \end{bmatrix}. \tag{42}$$

From Eq. (42) it is clear that when a $\sigma+2\pi$ sech pulse is used, there is actually some error in the rotation scheme of

the previous sections, due to an incomplete Rabi cycle involving the new state $|H\bar{l}\rangle$, and also due to some population transfer to the $|\bar{H}l\rangle$ state. Although this is going to be a very small effect (compared, for example, to the decay of the trion state during the pulse action), we can compensate for it by changing the polarization of the applied field and recover a 3×3 Λ system, which will allow us to use our rotation scheme, as proposed in Sec. V. To find the target polarization, we assume elliptical polarization

$$c_x\hat{x} + ic_y\hat{y} \tag{43}$$

and require

$$\langle \bar{H}l|(c_x\hat{x} + ic_y\hat{y})|\bar{z}\rangle = 0. \tag{44}$$

Solving Eq. (44) for the c's along with the normalization condition $c_x^2+c_y^2=1$, we find

$$c_x^0 = \frac{\frac{1}{\sqrt{2}}\cos\frac{\psi}{2} - \frac{1}{\sqrt{6}}\sin\frac{\psi}{2}}{\left(\cos^2\frac{\psi}{2} + \frac{1}{3}\sin^2\frac{\psi}{2}\right)^{1/2}}, \tag{45}$$

$$c_y^0 = \frac{\frac{1}{\sqrt{2}}\cos\frac{\psi}{2} + \frac{1}{\sqrt{6}}\sin\frac{\psi}{2}}{\left(\cos^2\frac{\psi}{2} + \frac{1}{3}\sin^2\frac{\psi}{2}\right)^{1/2}}. \tag{46}$$

Then a three-level system is recovered, consisting of the states $|z\rangle$, $|\bar{z}\rangle$, and $|H\bar{l}\rangle$, and our rotation scheme may be carried out.

To determine the desired polarization, knowledge of ψ, and thus c_x^0, c_y^0, is not necessary. Instead, a feedback loop can be devised, in the spirit of the one described in Sec. VIII A

The Hamiltonian for arbitrary elliptical laser polarization $c_x\hat{x}+ic_y\hat{y}$ is given by

$$H = \begin{bmatrix} 0 & \omega_B & \Omega_+ & 0 \\ \omega_B & 0 & 0 & \Omega_- \\ \Omega_+^* & 0 & \frac{\bar{\epsilon}}{2} - \lambda & 0 \\ 0 & \Omega_-^* & 0 & \frac{\bar{\epsilon}}{2} - \lambda \end{bmatrix}, \tag{47}$$

where

$$\Omega_+ = -\Omega\frac{(c_x + c_y)}{\sqrt{2}}\cos\frac{\psi}{2} - \Omega\frac{(c_x - c_y)}{\sqrt{6}}\sin\frac{\psi}{2}, \tag{48}$$

$$\Omega_- = \Omega\frac{(c_x - c_y)}{\sqrt{2}}\cos\frac{\psi}{2} + \Omega\frac{(c_x + c_y)}{\sqrt{6}}\sin\frac{\psi}{2}. \tag{49}$$

Initially the density matrix is taken to be in a spin ensemble $\rho=\mathrm{diag}(1/2,1/2,0,0)$. After the pulse we have $\rho=\mathrm{diag}\left(\frac{1}{2}\cos^2\frac{\theta_+}{2}, \frac{1}{2}\cos^2\frac{\theta_-}{2}, \frac{1}{2}\sin^2\frac{\theta_+}{2}, \frac{1}{2}\sin^2\frac{\theta_-}{2}\right)$, where $\theta_\pm = \frac{2\pi\Omega_\pm}{\sigma}$. The signal then, ignoring SGC, will be

$$P = \frac{A}{2}\left(\cos^2\frac{\theta_+}{2} - \cos^2\frac{\theta_-}{2}\right) = \frac{A}{4}(\cos\theta_+ - \cos\theta_-)$$
$$= -\frac{A}{2}\sin\frac{\theta_+ + \theta_-}{2}\sin\frac{\theta_+ - \theta_-}{2}.$$

Inserting the expressions for the angles $\theta_\pm$, we get

$$P = \frac{A}{2}\sin\left(\frac{2\pi\Omega}{\sigma}c_y\left[\frac{1}{\sqrt{6}}n\frac{\psi}{2} - \frac{1}{\sqrt{2}}\cos\frac{\psi}{2}\right]\right)$$
$$\times \sin\left(\frac{2\pi\Omega}{\sigma}c_x\left[\frac{1}{\sqrt{6}}\sin\frac{\psi}{2} + \frac{1}{\sqrt{2}}\cos\frac{\psi}{2}\right]\right)$$
$$\equiv \frac{A}{2}\sin(\alpha_1\pi c)\sin(\alpha_2\pi\sqrt{1-c^2}). \tag{50}$$

The feedback loop is designed as follows: First, we pick $c=c_x=1/\sqrt{5}$ and the signal is

$$P_1 = \frac{A}{2}\sin\left(\frac{\alpha_1\pi}{\sqrt{5}}\right)\sin\left(\frac{2\alpha_2\pi}{\sqrt{5}}\right). \tag{51}$$

For the second run, we choose $c\to 2c$ we get

$$\frac{P_2}{P_1} = \frac{\cos(\alpha_1\pi/\sqrt{5})}{\cos(\alpha_2\pi/\sqrt{5})}, \tag{52}$$

which after some algebra becomes

$$\frac{P_2}{P_1} = \frac{\cos(\alpha_1\pi/\sqrt{5})}{\cos\left(\frac{\alpha_1\pi}{2\sqrt{5}} + \sqrt{\frac{2\pi^2\Omega^2}{5\sigma^2} - \frac{3\alpha_1^2\pi^2}{20}}\right)}, \tag{53}$$

where

$$\alpha_1 = \frac{2\Omega}{\sigma}\left(\frac{1}{\sqrt{6}}\sin\frac{\psi}{2} + \frac{1}{\sqrt{2}}\cos\frac{\psi}{2}\right). \tag{54}$$

Equations (53) and (54) can be solved numerically and thus determine ψ, from which the target polarization will be found from Eqs. (45) and (46), so that in the third run the ideal polarization will have been reached.

For small angle ψ, i.e., small mixing, the small-angle approximation may be employed to obtain an analytical solution for the polarization of the third run in terms of the signals from the first two runs. In this limit, we have for α_1

$$\alpha_1 \approx \frac{2\Omega}{\sigma}\left(\frac{\psi}{2\sqrt{6}} + \frac{1}{\sqrt{2}}\right), \tag{55}$$

and ψ is then

$$\psi = \frac{\sqrt{30}\sigma}{\pi\Omega}\cot\left(\frac{2\pi\Omega}{\sqrt{10}\sigma}\right)\frac{P_1 - P_2}{P_1 + P_2}. \tag{56}$$

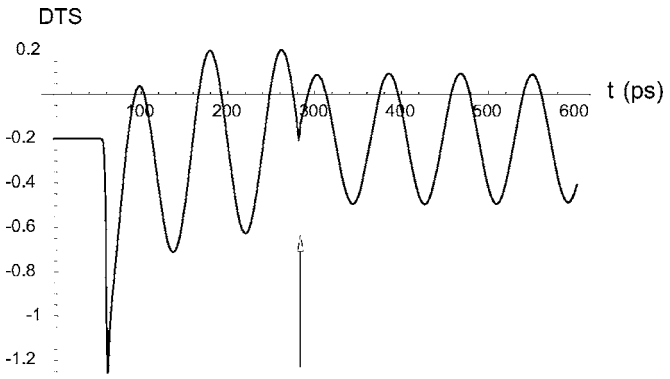

FIG. 16. DTS representing ensemble spin rotation by π using a resonant pulse with $\sigma=0.4$ meV. The fidelity of the rotation is a lot lower than the single-qubit case. The arrow indicates the time of incidence of the control pulse.

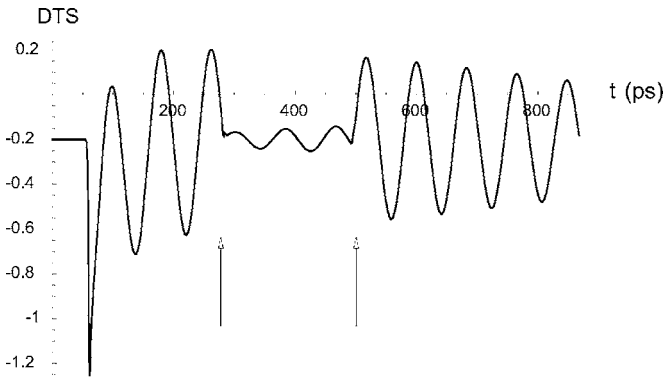

FIG. 17. DTS representing ensemble spin rotation by $\pi/2$. To demonstrate that the operation is a rotation, a second pulse is used to restore the beats. The two arrows indicate the incidence times of the two control pulses.

IX. ERRORS DUE TO INCOMPLETE RABI FLOP OF EXCITONS

A crucial feature in our scheme is the complete Rabi flop of the trion with a 2π pulse. Rabi oscillations for excitons in quantum dots have been demonstrated experimentally,[18] but they do exhibit distinct features compared to atoms. In Ref. 19 exciton population was measured as a function of the pulse area. For areas larger than π, the Rabi oscillations were shown to degrade considerably and the exciton was not flopped all the way back to the vacuum by a 2π pulse. This effect was seen by several groups,[19,20] and it was attributed to itinerant excitons, phonons, and coupling to wetting layer states.[21] Rabi oscillations between spins and trion states were demonstrated recently in ensemble experiments to have the same feature.[3] We note that for for practical use of our scheme this issue certainly has to be addressed, but for experimental demonstration the rotation should be evident (with a fidelity loss) even in the presence of the damped Rabi flop. In a future work, we will take into account the deteriorating mechanism and try to correct for it via pulse shaping and feedback loops.

X. ROTATIONS ABOUT OTHER AXES

A full set of rotations about one more axis would allow for an arbitrary rotation when combined with the rotations about z. Using the heavy-hole trion state, we can obtain rotations about x using again RZ pulses, albeit a lot slower ones, by frequency selectivity. If, e.g., a pulse is slow enough to excite only one of the two spin states along x, then a 2π RZ pulse, otherwise exactly the same as above, will cause a rotation about x. Clearly, we would have to pay the price of slow pulses, which is exactly what we set off to avoid. Possibly use of higher trion states (e.g., light hole trions) and/or tilting the optical axis away from z may allow for more efficient rotations about axes other than z.

XI. ENSEMBLE STUDY

The experiment may also be performed in an ensemble of dots. Both pump and probe pulses should be modulated at different frequencies,[22] whereas the control is left unmodulated, so that only the SV initialized by the pump is measured, and the control is measured to all orders in the control field.

In our simulations, we take into account the inhomogeneity of the g factors by an ensemble average over the Gaussian distribution with a full width at half maximum (FWHM) of $\Delta g=0.08g_0$,[1] and the inhomogeneity of the trion energies by a Gaussian, with a FWHM of about 3 meV.[23] The central spin Zeeman splitting is 50 μeV, so that it may represent GaAs dots in a high magnetic field. The pulse bandwidth is again chosen to be 0.3 meV. We have simulated the ensemble response for two different rotation angles, $\phi=\pi$, shown in Fig. 16 and $\phi=\pi/2$, shown in Fig. 17, cf to Figs. 5 and 8, respectively.

The first prominent feature of the plots is that the generated polarization drops by almost an order of magnitude compared to the single spin case. This is due to the contribution of the nonresonant dots to the beat signal. It also exhibits a spike, even for $\Omega=\sigma/2$. Moreover, the operation itself deteriorates significantly compared to the single dot, cf. Figs. 16 and 6 for example. However, the beat amplitude is found to be somewhat recovered by the second rotation in the $\phi=\pi/2$ case, and in the $\phi=\pi$ case, although the operation is far from unitary, the phase changes according to the theory. We therefore conclude that for demonstration purposes the ensemble should also work.

XII. CONCLUSIONS

We have shown how the analytically solvable sech pulses for a two-level system (Rosen-Zener pulses) may be used in a Λ type system when the two transitions share a common polarization and are close in frequency. The analyticity of the RZ pulses enables us to derive an analytical expression for the angle of rotation. Use of short pulses improves the fidelity of our scheme. Numerical simulation shows a fidelity of at least 96% for a realistic choice of parameters. Our scheme can be used to rotate about the growth direction the spin of electrons trapped in quantum dots via Raman transitions

involving the heavy hole trion. Thus, it does not supplant the full rotations in Ref. 8. However, it suggests the possibility for an experimental demonstration without need of addressing a single dot.

ACKNOWLEDGMENTS

This work was supported by ARO/LPS. S.E.E. acknowledges support from the Alexander S. Onassis Public Benefit Foundation.

*Present address: Naval Research Laboratory, Washington, DC 20375, USA.

[1] M. V. G. Dutt *et al.*, Phys. Rev. Lett. **94**, 227403 (2005).
[2] M. Atatüre, J. Dreiser, A. Badolato, A. Högele, K. Karrai, and A. Imamoglu, Science **312**, 551 (2006).
[3] A. Greilich *et al.*, Phys. Rev. Lett. **96**, 227401 (2006).
[4] J. G. Tischler, A. S. Bracker, D. Gammon, and D. Park, Phys. Rev. B **66**, 081310(R) (2002).
[5] M. Bayer, A. Kuther, A. Forchel, A. Gorbunov, V. B. Timofeev, F. Schäfer, J. P. Reithmaier, T. L. Reinecke, and S. N. Walck, Phys. Rev. Lett. **82**, 1748 (1999).
[6] M. Kroutvar, Y. Ducommun, D. Heiss, M. Bichler, D. Schuh, G. Abstreiter, and J. J. Finley, Nature (London) **432**, 81 (2004).
[7] Z. Kis and F. Renzoni, Phys. Rev. A **65**, 032318 (2002).
[8] P. Chen, C. Piermarocchi, L. J. Sham, D. Gammon, and D. G. Steel, Phys. Rev. B **69**, 075320 (2003).
[9] T. Calarco, A. Datta, P. Fedichev, E. Pazy, and P. Zoller, Phys. Rev. A **68**, 012310 (2003).
[10] S. E. Economou, L. J. Sham, Y. Wu, and D. G. Steel (unpublished).
[11] N. Rosen and C. Zener, Phys. Rev. **40**, 502 (1932).
[12] A. Bambini and P. R. Berman, Phys. Rev. A **23**, 2496 (1981).
[13] R. I. Dzhioev, V. L. Korenev, B. P. Zakharchenya, D. Gammon, A. S. Bracker, J. G. Tischler, and D. S. Katzer, Phys. Rev. B **66**, 153409 (2002).
[14] S. E. Economou, R.-B. Liu, L. J. Sham, and D. G. Steel, Phys. Rev. B **71**, 195327 (2005).
[15] M. E. Ware, E. A. Stinaff, D. Gammon, M. F. Doty, A. S. Bracker, D. Gershoni, V. L. Korenev, S. C. Bădescu, Y. Lyanda-Geller, and T. L. Reinecke, Phys. Rev. Lett. **95**, 177403 (2005).
[16] C. Piermarocchi, P. Chen, Y. S. Dale, and L. J. Sham, Phys. Rev. B **65**, 075307 (2002).
[17] J. F. Poyatos, J. I. Cirac, and P. Zoller, Phys. Rev. Lett. **78**, 390 (1997).
[18] T. H. Stievater, X. Li, D. G. Steel, D. Gammon, D. S. Katzer, D. Park, C. Piermarocchi, and L. J. Sham, Phys. Rev. Lett. **87**, 133603 (2001).
[19] Q. Q. Wang, A. Muller, P. Bianucci, E. Rossi, Q. K. Xue, T. Takagahara, C. Piermarocchi, A. H. MacDonald, and C. K. Shih, Phys. Rev. B **72**, 035306 (2005).
[20] A. Zrenner, E. Beham, S. Stufler, F. Findeis, M. Bichler, and G. Abstreiter, Nature (London) **418**, 612 (2002).
[21] J. M. Villas-Bôas, S. E. Ulloa, and A. O. Govorov, Phys. Rev. Lett. **94**, 057404 (2005).
[22] N. H. Bonadeo, J. Erland, D. Gammon, D. Park, D. S. Katzer, and D. G. Steel, Science **282**, 1473 (1998).
[23] J. Cheng, M. V. Gurudev Dutt, D. G. Steel, A. S. Bracker, D. Gammon, and L. J. Sham (unpublished).